

## A Two-Stage Sliding Window Method for Region-based Lung CT Image Retrieval

Ling Ma<sup>1</sup>, Xiabi Liu<sup>1</sup>, Chunwu Zhou<sup>2</sup>, Xinming Zhao<sup>2</sup>, Yanfeng Zhao<sup>2</sup>

<sup>1</sup>Beijing Laboratory of Intelligent Information Technology, School of Computer Science and Technology, Beijing Institute of Technology, Beijing 100081, China;

<sup>2</sup>Dept. of Imaging Diagnosis, Cancer Hospital, Chinese Academy of Medical Sciences, Beijing, China

**Abstract.** This paper proposes a novel two-stage sliding window method to retrieve lung CT images containing the regions that are visually similar with the query region. The method includes two stages. In the first stage, the sliding window technique and the Gray Level Co-Matrix (GLCM) based textural features are applied to obtain candidate retrieval results. In the second stage, the final results are selected from the candidate ones by using shape features based on Zernike moments. Via the two-stage processing, the similarity between regions can be measured more accurately and at the same time the algorithm can be performed efficiently. We tested the proposed two-stage sliding window method through conducting region-based image retrieval experiments on a set of 40 lung CT slices. The experimental results show that our method is effective and promising.

**Keywords:** medical image retrieval, lung CT images, sliding window, Gray Level Co-Matrix (GLCM), Zernike moments

### 1 Introduction

The content-based medical image retrieval (CBMIR) has attracted a lot of attention in recent years [1]. It can be an aid in the early diagnosis of disease to improve the quality of life of patients and reduce the mortality rate. Usually, the radiologists or physicians are interested in the local areas associated with the disease in the images, so it is important to retrieve the medical images according to the query regions indicated by the user.

The previous works for addressing the problem can be divided into two types. The first type of methods identifies the disease category of the query region. Then the images are retrieved by using the information of disease category. Aisen et al. [2] diagnosed the pathology bearing regions (PBR) into specific disease and retrieved all images that match the query image according to the image attributes determined previously to best characterize the diagnosed disease. Dy et al. [3] classified a query image into one of the disease categories, and then searched the similar images in the same class in terms of disease severity, stage, treatment, structure, and visual appearance. The methods based on disease category classification need sufficient examples

for training the classifiers, so the methods are not suitable to the situation where the query region is corresponding with some rare disease or signs. In the second type of methods, the regions of interests (ROI) in the database images are extracted. Then the images are retrieved according to the similarities between query region and ROIs. Kim et al. [4] compared the query region with the highlight regions segmented from the database images by their feature distance to choose the matched regions whose distances are minimum. Lam et al. [5] stored the lung CT images with nodule areas annotated by physicians. They used the different similarity measurements for different features to obtain the best retrieval result. Respectively, for Haralick features, they used distance measurements, including the Euclidean Distance, Manhattan Distance, and Chebyshev Distance, and for the Gabor and MRF feature vectors, they used the Chi-Squared Statistic and the Jeffrey Divergence. He et al. [6] extracted and stored the visual features of ROIs that be delineated by radiologists. By computing the similarity of features between the query ROI and the stored ROIs, the similar images were returned as search results. Obviously, the ROI extraction is crucial to the second type of methods. The failure of ROI extraction will leads to the error of image retrieval.

In this paper, we resort to sliding window technique [7] for solving the problem of region-based medical image retrieval and propose a corresponding two-stage method. The method computes the similarities between regions by using the Gray Level Co-Matrix (GLCM) based textural features and Zernike moments based shape features, respectively. In order to speed up the computation, the method is divided into two stages. In the first stage, we explore the regions in the database images by using the sliding window technique. The similarity between each explored region and the query region is measured based on the GLCM features. For each image in the database, the region corresponding to the maximum similarity is considered as the region matched with the query region. Then the candidate retrieval images are determined according to similarities of the matching regions. In the second stage, the similarities between the matching regions in the candidate results and the query region is further measured by using the Zernike moments based shape features and used to obtain the final result. We tested the proposed two-stage sliding window method for region-based lung CT image retrieval on a set of 40 lung CT slices. The 71.8% of precision rate and 61.67% of recall rate are achieved on the dataset, which show that our method is effective and promising.

## 2 The proposed method

The measurement of the similarity between regions is crucial to the region-based image retrieval. Combining multiple features is a reasonable strategy for dealing with this problem [8]. Texture, color, and shape are three main types of features used in the content-based image retrieval (CBIR). In the medical domain, color features are often of very limited expressive power. So we consider utilizing texture and shape features in this work.

The GLCM is a main tool in image texture analysis while Zernike moments have the desirable properties for describing the shape that are rotation invariance, robust-

ness to noise and expression efficiency. Both of them have already proved their abilities in the medical imaging applications, such as lung cancer disease diagnosis [9], lung nodule detection [10], mammography diagnosis [11], and etc. Therefore, we extract texture features and shape features of regions in the lung CT images by using these two techniques, respectively.

We consider using the two features and the sliding window technique to perform the region-based lung CT image retrieval. In order to improve the computation speed, the two features are employed in each of two stages, respectively. Firstly, the sliding window technique is used to explore the regions in each database image and the similarities between the regions and the query region are computed based on the GLCM features. Then the database images are ranked in descending order of the maximum region similarity for each of them. The top ranked images are taken as the candidate retrieval results. Finally, the Zernike moments based shape features are introduced to select the retrieved results from the candidate ones. Fig. 1 shows the flowchart of our proposed two-stage sliding window method for region-based lung CT image retrieval. The details of the processing in two stages are given in the following subsections.

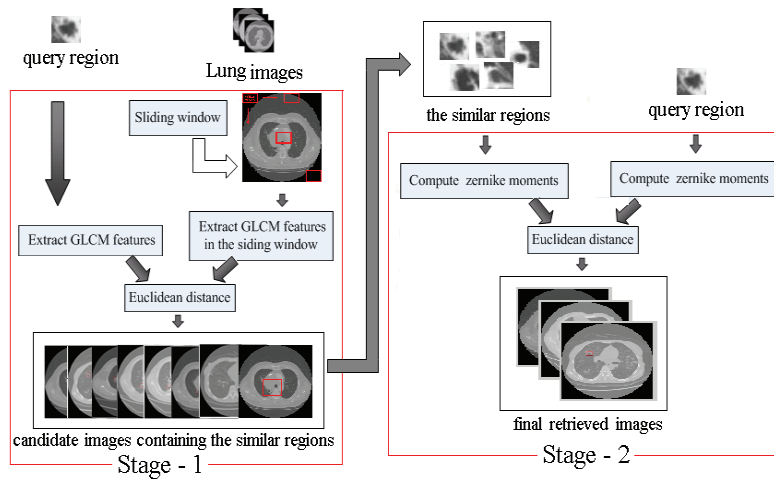


Fig. 1. The flowchart of the proposed two-stage sliding window method for region-based lung CT image retrieval

## 2.1 Stage-1:Preliminary retrieval

### 2.1.1 GLCM feature extraction

The lung CT image data is generally formatted as Digital Imaging and Communications in Medicine (DICOM) [12]. The range of gray level in the DICOM images is [-2048, 2047], which is compressed into 256 gray levels for accelerating the feature extraction procedure in this work.

On the transformed image with 256 gray levels, we construct the GLCM [13], based on which four features are extracted, including energy (a measure of homo-

generity of image), contrast (a measure of the contrast or the amount of local variations present in an image), entropy (a measure of the disorder of an image) and correlation (a measure of the regional pattern liner-dependencies in the image). The equations for computing four features are listed in Table 1, where  $P_{d,\theta}(i, j)$  is an element of a GLCM. In  $P_{d,\theta}(i, j)$ ,  $i$  is the gray level at location  $(x, y)$  and  $j$  is the gray level of neighboring pixel at a distance  $d$  and an orientation  $\theta$  from location  $(x, y)$ .

We construct the GLCM with a distance of one pixel and the four directions of  $0^\circ$ ,  $45^\circ$ ,  $90^\circ$  and  $135^\circ$ . Thus we get a 16-D GLCM feature vector to represent the query region and the regions in the database images.

**Table 1.** GLCM features used in this work

Energy	$\sum_i \sum_j P_{d,\theta}^2(i, j)$
Entropy	$-\sum_i \sum_j P_{d,\theta}(i, j) \log P_{d,\theta}(i, j)$
Contrast	$\sum_i \sum_j (i - j)^2 P_{d,\theta}(i, j)$
Correlation	$\frac{\sum_i \sum_j i \cdot j \cdot P_{d,\theta}(i, j) - u_i u_j}{\sqrt{(\sigma_i^2)(\sigma_j^2)}}$ <p>Where: <math>\sigma_i^2 = \sum_{i,j} (i - u_i)^2 \times P_{d,\theta}(i, j)</math>  <math>\sigma_j^2 = \sum_{i,j} (j - u_j)^2 \times P_{d,\theta}(i, j)</math>  <math>u_i = \sum_{i,j} i \times P_{d,\theta}(i, j)</math>  <math>u_j = \sum_{i,j} j \times P_{d,\theta}(i, j)</math></p>

### 2.1.2 Similarity metric

The similarity between two regions is measured by their Euclidean distance. Let  $V_i(k)$  be the  $k$ -th element in the 16-D GLCM feature vector of the  $i$ -th region. Then the distance between two regions is computed as

$$d_G = \sqrt{\sum_k (V_i(k) - V_j(k))^2}. \quad (1)$$

Obviously, the less the distance is, the larger the similarity is.

### 2.1.3 Sliding window search

We define a bounding rectangle as the sliding window, the size of which is the same as that of the query region. For each database image, starting from the top-left corner of the image, a sliding window moves with 3 pixels of sliding step horizontally and vertically through all the rows and columns of the image until the bottom-right corner is reached. At each rectangle region bounding in the sliding window, we extract the GLCM feature vector and calculate the distance between the region and the query region by using Eq. 1. Then the minimum distance between rectangle regions and the query region is determined for each database image. Finally, the database images are ranked in ascending order of their minimum region distance. The top  $N$  images are selected as the candidate retrieval results and the rectangle region corresponding to the minimum distance for each candidate result is recorded as the region matched with the query region.

## 2.2 Stage-2: Final retrieval

### 2.2.1 Zernike moments

Zernike moments [14, 15] are based on a set of complex polynomials that form a complete orthogonal set over the interior of the unit disk. Zernike moments are defined to be the projection of the image function on these orthogonal basis functions.

The basis computation function is

$$V_{n,m}(x, y) = V_{n,m}(\rho, \theta) = R_{n,m}(\rho) \exp(jm\theta), \quad (2)$$

where  $n$  is a non-negative integer,  $m$  is non-zero integer,  $\rho$  is the length of the vector from origin to point  $(x, y)$ ,  $\theta$  is the angle between the vector  $\rho$  and the x-axis in a counter clockwise direction and  $R_{n,m}(\rho)$  is the Zernike radial polynomial. In addition,  $n - |m|$  is even and  $|m| < n$ .

$R_{n,m}(\rho)$  in Eq. 2 is defined as:

$$R_{n,m}(\rho) = \sum_{k=|m|}^n \frac{(-1)^{\frac{n-k}{2}} \cdot \frac{n+k}{2}!}{\frac{n-k}{2}! \cdot \frac{m+k}{2}! \cdot \frac{k-m}{2}!} \rho^k = \sum_{k=|m|}^n \beta_{n,m,k} \rho^k. \quad (3)$$

Let  $V_{n,m}^*(x, y)$  be the complex conjugate of  $V_{n,m}(x, y)$ , then the Zernike moment of order  $n$  with repetition  $m$  for a digital image function  $f(x, y)$  is given by

$$Z_{n,m} = \frac{n+1}{\pi} \sum_{x^2+y^2 \leq 1} f(x, y) V_{n,m}^*(x, y). \quad (4)$$

Base on Eq. 2-4, 36 Zernike moments of order zero to ten are extracted from the image. Then we select the finally used features from these 36 Zernike moments. Actually, 20 Zernike moments of order 0 to 7 are selected by experiments in this paper.

### 2.2.1 Similarity metric

The similarity between two regions is calculated as the Euclidean distance between the two Zernike moments based feature vectors:

$$d_z = \sqrt{\sum_{i=0}^{L-1} (Z_q[i] - Z_p[i])^2}, \quad (5)$$

where  $L$  is the number of Zernike moments,  $Z_q[i]$  and  $Z_p[i]$  are the  $i$ -th moment of the query region and the matching region in the candidate retrieval results, respectively. After the distances based on the Zernike moments for all the candidate retrieval results are calculated by using Eq. 5, those candidate results with the distance less than a threshold value  $d_z^T$  will be selected as the final retrieval results. In this work, we set the value of  $d_z^T$  by careful experiments.

## 2.3 Experimental setup

In order to evaluate the proposed method, we conduct the experiments of region-based lung CT image retrieval on a set of 40 lung CT slices collected from a cancer hospital. The 30 slices in the dataset belong to three categories of imaging signs including lobulation, calcification and cavity. Each category of signs has ten slices,

respectively. The remaining 10 slices correspond to other signs. Each experimental image is of size  $512 \times 512$  pixels in DICOM standard. It should be noted that the sign category information is neglected in our method. We find out the images according to only visual similarity between regions.

The values of parameters in our method, including  $N$  in the first stage processing,  $n$  and  $d_z^T$  in the second stage processing, are set by careful experiments. The values of them leading to the results reported in the following section are:  $N = 15$ ,  $n = [0 - 7]$ ,  $d_z^T = 500$ .

## 2.4 Experimental results

We used the proposed method to perform the lung CT image retrieval by taking each of 30 slices belonging to the three categories of signs as the query image in which the user draw a rectangular query region. This means that the 30 rounds of query-by-region are conducted. We recorded the precision rate and recall rate for each query. The average precision rate and recall rate for each of the three sign categories and all the categories are calculated to evaluate the performance of our method, which are shown in Table 2.

**Table 2.** The precision rate and recall rate of our two-stage sliding window method

	<i>Overall</i>	<i>Lobulation</i>	<i>Calcification</i>	<i>Cavity</i>
precision rate	71.8%	66.7%	71.7%	77%
recall rate	61.67%	60%	50%	75%

Fig. 2 shows 3 examples of retrieval results, where the query images are shown in the left. From top to bottom, the query images are corresponding with the signs of lobulation, calcification and cavity, respectively. The small green rectangle in the query image is drawn by the user to indicate the lesion that he or she is interested in. The corresponding retrieved results are shown in the right column, where the small red rectangles are the regions which are matched with the query region. In order to display the content of the region more clearly, we magnify the query region and the matched regions and overlap them on the upper right of corresponding slices. The retrieved results are shown in descending order of the similarities, i.e, the ascending order of the distances, between the query region and matched regions from left to right and top to bottom. In these shown retrieved results, the irrelevant ones are indicated by the blue box and others are relevant.

As shown in Table 2 and Fig. 2, our method is effective, which achieved 71.8% of precision rate and 61.67% of recall rate, and the irrelevant images are usually ranked at the low position in the retrieval results. Table 2 also show that our method behaved best on the cavity category. The reasons are analyzed as follows. The size and shape of signs for cavity are more stable than those of lobulation and calcification. As shown in Fig. 2, the textural and shape features of the retrieved irrelevant results locating at the lung contour are very similar with those of the query regions for lobulations. Since the signs usually appear in the lung parenchyma, we can improve our method by extracting the pulmonary parenchyma and searching the similar regions in

the pulmonary parenchyma. As for calcification, from the Table 2, we find that the calcification has much lower recall rate (only 50%). Then we check the missing slices and find that they have a different size with that of the query region. As a result, they are filtered out in the stage-1 due to the fixed size of the sliding window. To solve this problem, we will extend our method to select optimal window sizes in the stage-1 in the future.

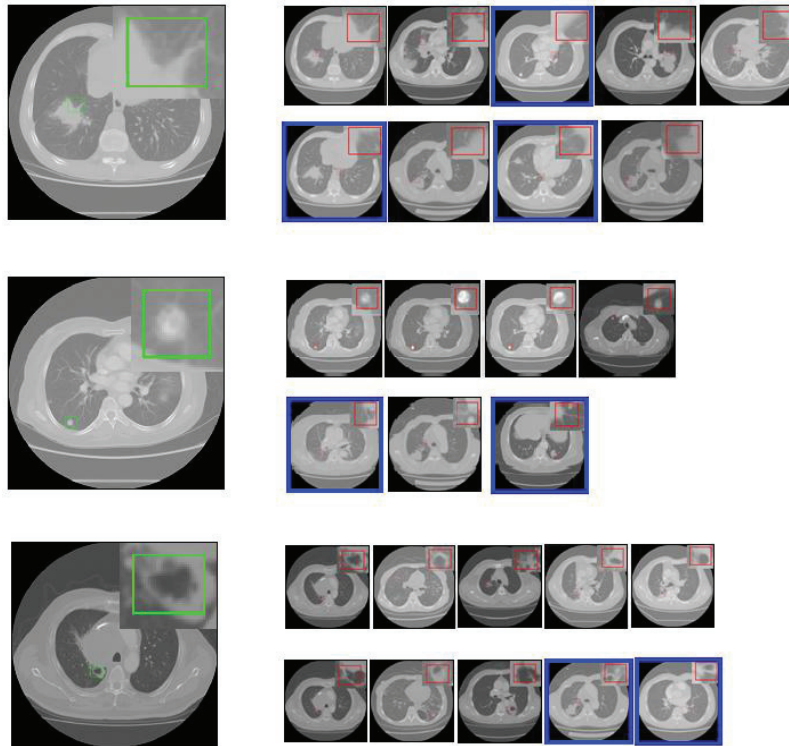


**Fig. 2.** The examples of lung CT image retrieved by our method: The three lung CT slices belonging to the three categories of signs and the query regions drawn by the user (left column); the retrieved results with matched regions (right column).

### 3 Conclusions

In this paper, a novel two-stage method for region-based lung CT image retrieval has been proposed based on the sliding window technique, the GLCM features and the Zernike moments. The main features of our methods are: 1) The sliding window technique is introduced into medical imaging community to find out the regions in database images which are similar with the query region; 2) The GLCM features and Zernike moments are merged in two-stage processing to achieve the tradeoff between the

retrieval effectiveness and the computation efficiency. Our method achieved the 71.8% of precision rate and 61.67% of recall rate on a set of 40 lung CT slices and the irrelevant images are usually ranked at the low position in the retrieval results, which shows that our method is effective and promising. The adaptive selection of sliding window sizes is still an open issue in the proposed approach, which will be explored in our future work.

#### Acknowledgements

This research was supported by National Natural Science Foundation of China (Grant no. 60973059, 81171407) and Program for New Century Excellent Talents in University of China (Grant no. NCET-10-0044)

#### Reference

1. H Müller, N Michoux, D Bandon, A Geissbuhler. "A review of content-based image retrieval systems in medical applications — clinical benefits and future directions". *International Journal of Medical Informatics*. Volume 73, Issue 1, February 2004, Pages 1–23.
2. AM Aisen, LS Broderick, H Winer-Muram . CE Brodley, AC Kak, C Pavlopoulou, et al. "Automated storage and retrieval of thin-section CT images to assist diagnosis: system description and preliminary assessment". *Radiology*. 2003 Jul, 228(1):265-70.
3. JG Dy, CE Brodley, A Kak , LS Broderick, AM Aisen. "Unsupervised Feature Selection Applied to Content-Based Retrieval of Lung Images". *IEEE Transactions on Pattern Analysis and Machine Intelligence*, v.25 n.3, p.373-378, March 2003.
4. E Kim, S Antani, X Huang, LR Long, D Demner-Fushman. "Using relevant regions in image search and query refinement for medical CBIR", *Conference on Medical Imaging - Advanced PACS-based Imaging Informatics and Therapeutic Applications, Proceedings of the SPIE*, Volume 7967, pp: 796707.1-796707.8, March 2011.
5. MO Lam, T Disney, DS Raicu, J Furst, DS Channin. "BRISC—an open source pulmonary nodule image retrieval framework". *Journal of Digital Imaging*, 20 (1) (2007), pp. 63–71.
6. Z He, Y Zhu, T Ling et al. "Combining Text Retrieval and Content-based Image Retrieval for Searching Large-scale Medical Image Database in Integrated RIS/PACS Environment" *SPIE 2009* ,Vol. 7264 72640U-1-9.
7. D. Iakovidis , N. Pelekis , E. Kotsifakos , I. Kopanakis , H. Karanikas and Y. Theodoridis "A pattern similarity scheme for medical image retrieval", *IEEE Trans. Inf. Technol. Biomed.*, vol. 13, no. 4, pp.442 -450 2009.
8. XY Wang, YJ Yu, HY Yang. "An effective image retrieval scheme using color, texture and shape features", *Computer Standards & Interfaces*, Volume 33 Issue 1, pp. 59-68, January, 2011.
9. P Paulus, FL Gaol. "Lung Cancer Diseases Diagnostic Assistance Using Gray Color Analysis". *Computational Intelligence, Modelling and Simulation (CIMSIM)* , pp. 355- 359. Sept. 2010.
10. CZ Shi, Q Zhao, LP Luo. "Application of Gray-Scale Texture Feature in the Diagnosis of Pulmonary Nodules". *Applied Mechanics and Materials*, Vol. 140, pp. 34-37, November, 2011.
11. A Tahmasbi, F Saki, SB Shokouhi. "Classification of benign and malignant masses based on Zernike moments" *J. Computers in Biology and Medicine*, vol. 41, no. 8, pp. 726-735, 2011.
12. MI Rajab, AA Eskandar. "Enhancement of radiographic images in patients with lung nodules". *Thoracic Cancer*. Volume 2, Issue 3, pages 109–115, August 2011.
13. RM Haralick, K Shanmugam, IH Dinstein. "Texture features for image classification" [J]. *IEEE Trans on Systems, Man, and Cybernetics*, 1973, 3(6): 610- 621.
14. G. Amayeh , A. Erol , G. Bebis and M. Nicolescu. "Accurate and efficient computation of high order Zernike moments", *Proc. 1st Int. Symp. Vision and Computation*, p.462 , 2005.
15. WY Kim, YS Kim. "A region-based shape descriptor using Zernike moments". *Signal Process. Image Commun*, 16 (2000), pp. 95–102.